Table 1. The values of annealing rate, V_a, as the rate of change of length and diameter, for different angles θ of incident beam (^{208}Pb at 17 MeV n^{-1}), annealed for 10 min

Serial No.	T (°C)	T (K)	$\frac{10^3}{T}$ (K^{-1})	$\theta = 90°$: D (μm)	$\theta = 90°$: $V_a = \frac{dD}{dt}$	$\theta = 45°$: Observed length l' (μm)	$\theta = 45°$: Actual length $l'/\cos\theta$	$\theta = 45°$: $V_a = \frac{dl}{dt}$	$\theta = 45°$: D (μm)	$\theta = 45°$: $V_a = \frac{dD}{dt}$
1	Unannealed	—	—	17.50 ± 0.20*	—	20.00 ± 0.25	28.17†	—	11.00 ± 0.15*	—
2	50	323	3.09	16.25 ± 0.15	0.12	18.50 ± 0.15	26.05	0.21	10.00 ± 0.10	0.10
3	100	373	2.68	15.00 ± 0.12	0.25	16.50 ± 0.15	23.24	0.49	8.50 ± 0.15	0.25
4	150	423	2.36	13.50 ± 0.15	0.40	14.00 ± 0.20	19.72	0.85	6.50 ± 0.10	0.45
5	200	473	2.11	10.00 ± 0.10	0.75	10.00 ± 0.10	14.08	1.41	4.00 ± 0.12	0.70
6	250	523	1.91	6.50 ± 0.15	1.10	5.00 ± 0.10	7.04	2.11	1.00 ± 0.10	1.00

*D_0.
†l_0.

etched along with the parent unannealed sample, under the optimum etching conditions of 2.5% HF at room temperature (32°C) with etching time varying from 20 to 60 min.

The mean observed track lengths (l') and diameters (D) were measured using a Carl Zeiss microscope with a resolution of 1 μm. The actual mean lengths were calculated using the relation $l = l'/\cos\theta$, where θ is the angle of incident beam with respect to the detector surface. Statistical errors were also applied to these measurements for each ion set, they were also made to conform to a standard deviation of 1σ. The track etch rate, V_T, is obtained from the linear portion of the plot of track length vs etching time. The general etch rate, V_G, is found to be independent of the extent of annealing, and hence can be treated as constant for soda-lime glass. We have projected here the curves obtained from the annealing data for only the ^{139}La (14.6 MeV n^{-1}) ion beam, whereas the results for ^{208}Pb (17 and 13.6 MeV n^{-1}) ion beams have been tabulated, as the curves drawn for these ions show correspondence with those for ^{139}La.

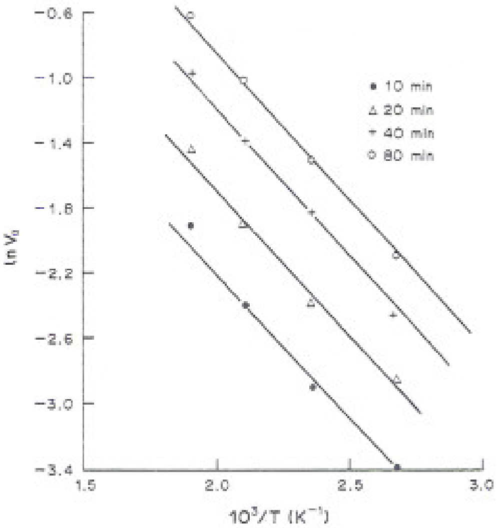

FIG. 1. Plot of ln V_a vs $1/T$ (10^3 K^{-1}) for a soda-lime glass detector using ^{139}La ions.

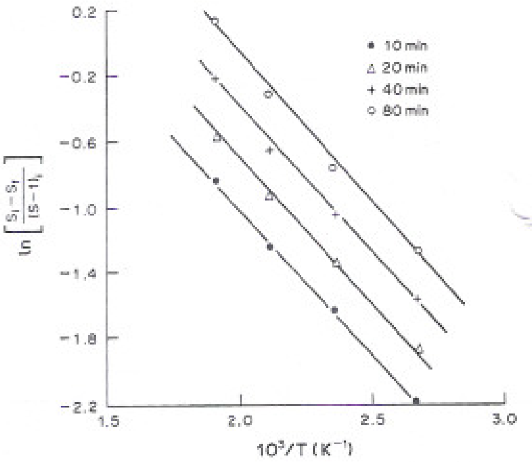

FIG. 2. Plot of ln $[(S_i - S_f)/(S - 1)_i]$ vs $1/T$ (10^3 K^{-1}) for a soda-lime glass detector using ^{139}La ions.

3. RESULTS AND DISCUSSION

The annealing rate, V_a, for different ion sets was calculated as the rate of change of length as well as diameter (Table 1). The plot of ln V_a against reciprocal temperature, T, yields a straight line for each ion

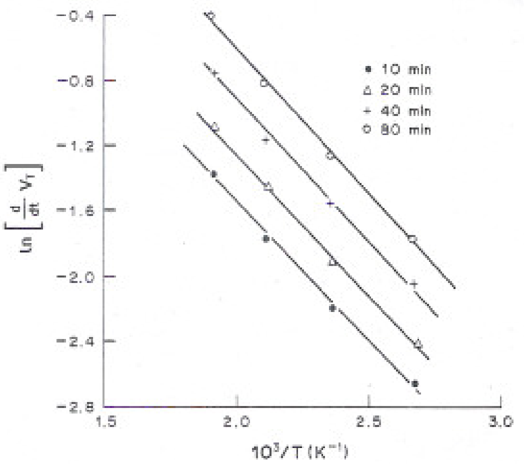

FIG. 3. Plot of ln $[d/dt\,(V_T)]$ vs $1/T$ (10^3 K^{-1}) for a soda-lime glass detector using ^{139}La ions.

Table 2. Comparison of E_a, n and A values obtained by using different formulations (see text)

	Modgil and Virk formulation			Price *et al.* formulation			Modified formulation of Modgil and Virk		
Ion beam	Activation energy E_a (eV)	n value	A value (μm min^{-1})	Activation energy E_a (eV)	n value	A value (μm min^{-1})	Activation energy E_a (eV)	n value	A value (μm min^{-1})
^{139}La (14.6 MeV n^{-1})	0.16	0.64	76–88	0.15	0.55	4.0–4.5	0.15	0.55	2.4–2.7
^{208}Pb (17 MeV n^{-1})	0.16	0.65	75–90	0.15	0.57	5.2–5.6	0.15	0.58	3.5–4.0
^{208}Pb (13.6 MeV n^{-1})	0.16	0.60	73–90	0.15	0.52	3.1–3.7	0.15	0.54	2.8–3.2

set (Fig. 1). The activation energy as calculated using equation (1) is 0.16 eV for all three ions.

Using the Price *et al.* (1987) formulation, the etch-rate ratio, $S = V_T/V_G$, is calculated for all three ions. The plots of the logarithms of the left-hand side of equation (2) against the reciprocal temperature yield straight lines (Fig. 2), and hence a single activation energy. This activation energy turns out to be identical (i.e. 0.15 eV) for all three ions, and thus appears to be only medium-specific. The annealing data for track etch rate, V_T, are also used to fit equation (3). The plot of the logarithm of the left-hand side of equation (3) against the reciprocal temperature again yields a straight line (Fig. 3) and, hence, a single activation energy of 0.15 eV.

Table 2 shows a comparison of values of E_a, n and A for all three ions, using different formulations. Thus, we find that our annealing data for soda-lime glass, using different formulations, give similar results for activation energy, E_a. However, A and n values are found to be quite discordant in these formulations.

The above results further support the concept of a single activation energy as an intrinsic property of the detector. It also proves that in those SSNTDs where general etch rate (V_G) is independent of annealing, our revised formulation is simpler and more suitable.

REFERENCES

Dakowski M. (1978) Length distributions of fission tracks in thick crystals. *Nucl. Track Detection* **2,** 181–189.

Dakowski M., Burchart J. and Gałązka J. (1974) Experimental formula for thermal fading of fission tracks in minerals and natural glasses. *Bull. Acad. pol. Sci. Sér. Sci. Terre* **22,** 11–17.

Dartyge E., Daraud J. P., Langevin Y. and Maurette M. (1981) New model of nuclear particle tracks in dielectric minerals. *Phys. Rev.* **B23,** 5213–5229.

Durrani S. A. and Khan H. A. (1970) Annealing of fission tracks in tektites: corrected ages of bediasites. *Earth Planet. Sci. Lett.* **9,** 431–445.

Gold R., Roberts J. H. and Ruddy F. H. (1981) Thermal fading of latent tracks of iron nuclei in lexan polycarbonate. *Nucl. Tracks Radiat. Meas.* **5,** 251–256.

Mantovani M. S. M. (1974) Variations of characteristics of fission tracks in muscovites by thermal effects. *Earth Planet. Sci. Lett.* **24,** 311–316.

Märk E., Pahl M., Purtscheller E. and Märk T. D. (1973) Thermische Ausheilung von Uran-Spaltspuren in Apatiten, Alterskorrekturen und Beitrage zur Geothermochronologie. *Tschermaks miner. petrpogr. Mitt.* **20,** 131–154.

Märk T. D., Pahl M. and Vartanian R. (1981) Fission track annealing and fission track–temperature relationship in sphere. *Nucl. Technol. Ser.* **52,** 295–305.

Modgil S. K. and Virk H. S. (1984) Track annealing studies in glasses and minerals. *Nucl. Tracks Radiat. Meas.* **8,** 355–360.

Modgil S. K. and Virk H. S. (1985) Annealing of fission fragment tracks in inorganic solids. *Nucl. Instrum. Meth.* **B12,** 212–218.

Naeser C. W. and Faul H. (1969) Fission track annealing in apatite and sphene. *J. geophys. Res.* **74,** 705–710.

Price P. B., Gerbier G., Park H. S. and Salamon M. H. (1987) Systematics of annealing of tracks of relativistic nuclei in phosphate glass detectors. *Nucl. Instrum. Meth.* **B28,** 53–55.

Reimer G. M., Wagner G. A. and Carpenter B. S. (1972) The thermal stability of fission tracks in the standard reference material glass standard. *Radiat. effects* **15,** 273–274.

Salamon M. H., Price P. B. and Drach J. (1986) Thermal annealing of nuclear tracks in polycarbonate plastic. *Nucl. Instrum. Meth.* **B17,** 173–176.

Storzer D. and Wagner G. A. (1969) Correction of thermally lowered fission track ages of tektites. *Earth Planet. Sci. Lett.* **5,** 463–468.

Virk H. S., Modgil S. K. and Singh G. (1987) Fission track annealing models and the concepts of a single activation energy. *Nucl. Instrum. Meth.* **B21,** 68–71.